Hindawi
Journal of Nanotechnology
Volume 2021, Article ID 5525690, 13 pages
https://doi.org/10.1155/2021/5525690

Research Article

Anticancer and Antimicrobial Activity Evaluation of Cowpea-Porous-Starch-Formulated Silver Nanoparticles

Shiara Ramdath, John Mellem, and Londiwe Simphiwe Mbatha

Department of Biotechnology and Food Science, Faculty of Applied Sciences, Durban University of Technology, P.O Box 1334, Steve Biko Campus, Durban 4000, South Africa

Correspondence should be addressed to Londiwe Simphiwe Mbatha; londiwem3@dut.ac.za

Received 4 February 2021; Accepted 3 May 2021; Published 10 May 2021

Academic Editor: Brajesh Kumar

Health issues involving inadequate treatment of diseases such as cancer and microbial infections continue to be the subject of much ongoing recent research. Biosynthesized silver nanoparticles (AgNPs) were characterized using Transmission Electron Microscopy (TEM), Zeta Sizer, Ultraviolet (UV), and Fourier Transform Infrared (FTIR) spectroscopy. Their antimicrobial activity was evaluated on selected Gram-positive and Gram-negative bacterial strains, using the disc diffusion and broth dilution assays. Cell viability profiles were evaluated using MTT (3-(4,5-dimethylthiazol-2-yl)-2,5-diphenyltetrazolium bromide) and apoptosis studies on selected human noncancer and cancer cells. The biosynthesized AgNPs were evaluated to be spherical clusters, with sizes between 40 and 70 nm. The absorption peak at 423 nm and the presence of polyphenols confirmed the synthesis and stabilization of these tested AgNPs. The AgNPs showed a good stability of -23.9 ± 1.02 mV. Good antimicrobial activity (6.0–18.0 mm) was seen on all tested bacteria at a minimum inhibitory concentration (MIC) ranging from 5 to 16 μg/ml, with the highest activity seen against Gram-negative *Escherichia coli* (18 ± 0.5 mm), and the lowest activity was seen against Gram-positive *Listeria monocytogenes* (6.0 ± 0.4 mm) after treatment with the AgNPs. These NPs showed a concentration-dependent and cell-specific cytotoxicity with low IC_{50} values (41.7, 56.3, and 63.8 μg/ml). The NPs were well tolerated by tested cells as indicated by a more than 50% cell viability at the high dose tested and low apoptotic indices (<0.2). These findings indicated that these biosynthesized AgNPs showed great potential as effective antibacterial agents and anticancer drug delivery modalities.

1. Introduction

Over the recent decades, various diseases from minor infections to severe cancer have persisted in posing serious worldwide health issues that urgently need prompt addressing [1]. To date, cancer is one of the most widely spread and diagnosed diseases worldwide and has been reported to be the leading cause of death in our modern society [2]. Current conventional treatments using synthetic generic drugs, surgery, radiation therapy, hormone therapy, and chemotherapy have proven ineffective in treating cancer [3, 4]. Microbial infections, on the other hand, are also now posing major health problems, especially in developing countries. Available synthetic antibiotics that are used against these microbial infections usually lead to antibiotic resistance after repeated use, hence rendering the drugs inadequate [5]. Hence, this demands that a renewed effort be made to seek new materials/agents which are cheap and are highly efficient in treating these diseases. Recent research advancements have focused on the production of nanocomposites or metal nanoparticles made with natural biomolecules (e.g., polymers) as potential alternative anticancer and antimicrobial modalities [6].

Silver nanoparticles (AgNPs) are one of the most researched metal nanoparticles and have been the subject of interest due to their remarkable physicochemical properties, particularly their large surface area, tunable size, and stability [7]. Their application has been greatly demonstrated in a range of fields such as pharmaceuticals, medicine, and biotechnology [7–9]. These NPs are particularly well known

for their antimicrobial activity, which is said to be attributed to the electrostatic interaction that occurs between the negatively charged cell membrane of microorganisms and the positively charged AgNPs [10, 11]. The accumulation of these NPs on the cell membrane is believed to alter the membrane causing it to lose permeability which leads to cell death [12]. However, due to toxic chemical agents used when preparing these NPs which affect their biocompatibility and pose environmental problems, biosynthesized AgNPs have been the subject of research recently. The biosynthesis of AgNPs involves a simple one-pot synthesis approach in which silver salts are reduced to fabricate AgNPs using nontoxic and natural polymers such as bacterial biomass, chitosan, and carbohydrates (e.g., starch) as both reducing and stabilizing agents [13,14].

For this experiment, colloidal AgNPs were prepared using porous cowpea starch. Cowpea (*Vigna unguiculata* L. Walp) is an annual plant legume that is cultivated and consumed mostly in South America, Asia, and Africa. Cowpea seed grains predominantly consist of bioactive compounds such as starch (35.0–52.0%), proteins (27%), and phenolic compounds (including phenol acids, flavonoids, and tannins) [15, 16]. These bioactive compounds are of great benefit to humans due to their anticarcinogenic effects and antioxidant and anti-inflammatory properties [17, 18]. Starch is the major dietary source of carbohydrates [19, 20]. It is a readily available biopolymer that possesses aldehyde terminals with hydroxyl groups capable of reducing silver nitrate ($AgNO_3$) to silver metal while simultaneously stabilizing the resulting NPs [7]. These hydroxyl groups further enable good shape, size, and dispersion tunability which in turn enhance the biodegradability and biocompatibility of the NPs [21]. In 2018, starch was officially accepted by all major regulatory agencies for use in various oral drug delivery systems [22, 23]. Porous starch, in particular, has an important role in drug delivery since it processes all the properties that an ideal drug/gene delivery system should have which includes, inertness, biocompatibility, bioadhesiveness, high drug loading capacity, and amenability to synthetic modification, e.g., addition of biodegradable targeting ligands such as folic acid, for targeted delivery [22]. In cowpea grains, starch is the most abundant carbohydrate, and when extracted, it is extremely small and porous which is an advantage in drug/gene delivery system design applications.

Hence, this study aims at investigating the antibacterial and anticancer profiles of cowpea-porous-starch-mediated AgNPs for potential application as anticancer drug delivery modalities or antimicrobial agents.

2. Experimental

2.1. Materials. Human breast adenocarcinoma cells (MCF-7), human alveolar basal epithelial adenocarcinoma cells (A549), and human embryonic kidney cells (HEK293) were obtained from the Department of Biological Sciences at the University of KwaZulu Natal (Westville campus). Minimum Essential Medium (EMEM) containing Earle's salts and L-glutamine, penicillin (500 units/ml)/streptomycin (5000 μg/ml), trypsin-versene, foetal bovine serum (FBS), benzolylated dialysis tubing (MWCO 12000 Da), and MTT were purchased from Sigma-Aldrich (St Louis, MO, USA). Mueller Hinton Broth (MHB) and Mueller Hinton Agar plates and microtiter plates were purchased from Bio-Rad Laboratories (Richmond, VA, USA). Microbank vials were purchased from Davies Diagnostic (SA). Bacterial cultures were obtained from Lancet Laboratories (SA). All other chemicals were of analytical grade and were supplied by Sigma-Aldrich (St Louis, MO, USA).

2.2. Methods

2.2.1. Starch Extraction. Starch extraction from the defatted flour was performed as described in [24] with slight modifications. Briefly, 100 g of cowpea starch was mixed with sodium borate buffer (12.5 mM, pH 10, 0.5% sodium dodecyl sulfate (SDS) (w/v) and 0.5% $Na_2S_2O_5$ (w/v)) on a stirrer for 5 minutes, followed by 10 minutes' centrifugation at 10,000×g to extract the proteins and recover the resultant residue. This was repeated 2X, and the resultant residue was washed 3X with distilled water and each time recovered by centrifugation. Thereafter, the residue was resuspended in distilled water and left overnight stirring to further extract the protein from the starch. Afterward, the starch slurry was filtered by passing through multilayers of cheesecloth and, thereafter, through a 250 μm sieve. This was then centrifuged at 10,000×g for 10 minutes, and thereafter, the brown layer formed on top of the starch layer was scraped with a spatula. Then, the starch was resuspended in water and centrifuged again, and this was repeated until all the brown particles were removed from the starch.

2.2.2. Preparation of Starch-Formulated/-Mediated AgNPs. AgNPs were prepared as previously described [25]. Briefly, 1.0 g of starch was mixed with 100 ml of deionized water and heated to 60°C on a hotplate with gentle stirring. Thereafter, 10 ml of starch solution was added with stirring to 50 ml of 1 mM $AgNO_3$ solution, and the reaction process was carried out in dark for 3 hours until a clear brown colour was evident which indicated the formation of the AgNPs. Finally, the resultant AgNP solution was then dialyzed to remove excess unreacted by-products against 18 M Ohm water for 24 hours using a dialysis tube size of MWCO 12,000 Dalton. Different concentrations of AgNPs were prepared by adjusting the $AgNO_3$ concentration.

2.2.3. Characterization of the Synthesized Nanoparticles

(1) UV Spectroscopy, TEM, SEM, ZetaPotential, and FTIR Spectroscopy. The formation of AgNPs was spectroscopically verified by using a UV-visible (vis) spectrophotometer (Cary 60 UV-Vis). The morphology and size of the AgNPs were determined using a JEOL JEM-1010 Transmission Electron Microscope with a Megaview III camera and iTEM UIP software (Tokyo, Japan) accessed from the University of Kwa-Zulu Natal (UKZN) (Westville Campus, South Africa).

A FEI XL30 Scanning Electron Microscope accessed from the UKZN was used to evaluate the shape of the starch. The *zeta* potential was determined using a *Zeta* Sizer (Anton Paar, Particle analyser, Litesizer 500). The conjugation of the functional groups on starch and AgNPs was investigated using a Spectrum 100 FTIR spectrophotometer (PerkinElmer Co., Ltd., MA, USA) accessed from UKZN (Westville Campus, South Africa).

2.2.4. Bacterial Cultures and Maintenance. Four bacteria were used and divided into Gram-negative (*Escherichia coli* ATCC 25922 and *Klebsiella pneumoniae* ATCC 31488) and Gram-positive (*Listeria monocytogenes* and *Staphylococcus aureus* ATCC 25923) strains. Bacterial cultures were maintained as previously described [26]. Initially, all bacterial cultures were plated out, verified using the Gram-staining procedure, and stocked in microbank vials using 50% glycerol. Then, when needed, these were grown in MHB for 24 hours at 37°C, and the absorbance of bacterial cells was adjusted to the MacFarland Standard of 0.5 which corresponds to 10^8 CFU/ml and the density measured was at a wavelength of 600 nm [27, 28].

2.2.5. Antibacterial Activity of the Porous-Starch-Formulated/-Mediated AgNPs. Antibacterial activity of porous starch-mediated AgNPs was assessed against Gram-negative and Gram-positive bacterial strains by agar disk diffusion assay as previously described [29]. Initially, the required nutrient media for all bacterial strains were prepared from Mueller Hinton agar, and 100 μl inoculums of each tested bacterial culture were swabbed onto agar plates and incubated at 37°C for 30 minutes. Thereafter, different concentrations of AgNPs sample solutions (1, 5, and 10 Molar) were pipetted onto 5.5 mm sterile Whatman No. 1 filter paper disks and then placed on the surface of the bacteria-treated plates. After a 24 hours' incubation period at 37°C, the diameter of the zone of inhibition was measured. Control disks with starch only (10 Molar) served as the negative control, whilst those with antibiotic ciprofloxacin (10 Molar) served as the positive control. All tests were carried out in triplicate.

2.2.6. Determination of MIC. Microtiter plates were used to evaluate the MIC values for AgNP sample solutions with bacteria activity. Briefly, on the microplates, serial dilutions ranging from 0.1 to 500 μg/ml of each concentration of AgNPs were performed. Then, inoculums of bacterial cultures (100 μl) were added to each well except the sterility controls, and then, the plates were incubated at 37°C for 24 hours. Following this, 50 μl of 2 μg/ml growth indicator p-iodonitrotetrazolium was added to each well and the incubation continued for 30 minutes. Starch was used as a negative control; MHB was used as a sterility control, and MHB + test bacteria served as the growth control. Growth was indicated by violet-coloured suspensions, while growth inhibition was indicated by colourless suspensions [29].

2.2.7. Cell Culture and Maintenance. Cells were grown at 37°C and 5% CO_2, in 25 cm^2 flasks with a sterile medium (EMEM) with (FBS 10% v/v, medium, streptomycin sulphate (100 μg/ml), and penicillin G (100 U/ml)). These were then subcultured when necessary [30].

2.2.8. Cytotoxicity Profile Study. To determine the cytotoxic activity of the AgNPs and the starch on selected cell lines, an MTT assay was used [2,30]. Briefly, cell lines HEK293 (human embryonic kidney), A549 (human alveolar basal epithelial adenocarcinoma), and MCF-7 (human breast adenocarcinoma) were trypsinised and seeded at densities of 1.62×10^6, 1.93×10^6, and 1.72×10^6 cells/well, respectively, in 96-well plates and incubated for 24 hours at 37°C. After incubation, old media were replaced with new media (0.3 ml), AgNPs and starch solutions prepared at different concentrations of 4, 7, 11, 15, and 19 Molar were added, and the cells were incubated for a further 48 hours at 37°C. Then, the old medium was replaced with fresh medium+10% MTT solution (5 mg/ml in PBS) and then incubated for 4 hours at 37°C. The medium + MTT solution was then removed, and cells were washed with PBS (2×0.3 ml) followed by treatment with DMSO (0.3 ml). Absorbance measurements were recorded at 570 nm. Cell viability was related to the control of untreated cells (100%). The average absorbance values were converted into percentage cell viability, using the following equation:

$$\text{Cell Viability (\%)} = \frac{\text{Average Absorbance (control)}}{\text{Average Absorbance (sample)}} \times 100. \quad (1)$$

IC_{50} values were determined by nonlinear regression based on the percentage cell viability vs. concentration of samples (μg/ml) plots (Figure S1), and these values represented the sample concentration needed to kill 50% of the tested cells.

2.2.9. Apoptosis Studies. To further evaluate the cell viability profile of the synthesized NPs, an apoptosis study was conducted as previously described [31]. At the onset, the HEK293, A549, and MCF-7 cells with densities of 1.62×10^6, 1.93×10^6, and 1.72×10^6 cells/well, respectively, were seeded into 12-well plates and incubated for 24 hours at 37°C. After incubation, AgNP and starch solutions of 10 Molar were separately added into the cells and then incubated for a further 24 hours at 37°C. Thereafter, the old media were removed, and the cells were washed with PBS (100 μl) and then stained with 10 μl of acridine orange/ethidium bromide (AO/ETBR) dye (100 μg ml^{-1} acridine orange and 100 μg ml^{-1} ethidium bromide). Finally, a fluorescent microscope (OLYMPUS) at ×200 magnification was used to study the morphological changes in the cells. The apoptotic index was calculated as follows:

$$\text{Apoptotic Index (AI)} = \frac{\text{Number of Apoptotic Cells}}{\text{Total Number of Cells}}. \quad (2)$$

2.2.10. Statistical Analysis. Antibacterial activity, cytotoxicity, and apoptosis studies were performed in triplicate, and the results were expressed as mean ± standard deviation (S.D). Data were analysed by one-way ANOVA and Tukey's multiple comparison test to compare between the groups. Statistically significant values are indicated by $^{*}p < 0.05$, $^{**}p < 0.01$, $^{***}p < 0.001$, and $^{****}p < 0.0001$.

3. Results and Discussion

3.1. Synthesis and Characterization

3.1.1. Synthesis and UV Spectroscopy Analysis. Metal nanoparticles are well known for their unique properties, particularly optical, as a result of surface plasmon resonance (SPR) [32]. Hence, the formation of the synthesized AgNPs was verified by observing colour change and UV-vis spectroscopy. The AgNPs prepared by mixing starch extracted from cowpea with $AgNO_3$ solution were successfully synthesized. This was indicated by the colour change of the reaction mixture from a colourless solution to a brown solution (Figures 1(a) and 1(b)). The colour change can be attributed to the reduction of silver ions (Ag^{+}) from silver nitrate into AgNPs by active biomolecules present in the starch extract [7]. The colour of AgNPs is due to the excitation of SPR arising due to the collective oscillation of free conduction electrons induced by an interacting electromagnetic field [33, 34]. Starch is said to peak between 200 nm and 250 nm [35]; hence, the peak at 230 nm showed its presence. Furthermore, the characteristic absorption band of AgNPs is known to range between 400 nm and 500 nm [36, 37]. The absorption observed at 423 nm (Figure 1(c)), thus, confirmed the successful preparation of AgNPs by the starch extract.

3.1.2. FTIR Spectroscopy Analysis. To identify the major functional groups present on the starch extract surface and their participation in the coating and stabilization of the AgNPs, FTIR analysis was carried out (Figure 2). Even though the mechanism of the reduction of silver ions to AgNPs is not exactly understood but postulated, comparing the FTIR spectra of the starch extract and that of the synthesized AgNPs results may shed some light with regards to whether the formulation was successful or not. Figure 2 shows the spectra of cowpea starch extract (a) and AgNPs formed with cowpea starch extract (b). From this, it can be seen that the spectrum of the starch extract matches very well with that of the synthesized AgNPs with a slight shift in peak positions and a decrease in intensity. The starch extract in Figure 2(a) showed characteristic intensity peaks at 3272 cm^{-1} assigned to O-H of alcohols from phenols, 2333 cm^{-1} and 2114 cm^{-1} assigned to C=C-C alkyne groups, 1635 cm^{-1} assigned to the N-H amine group, and 1151 cm^{-1}, 1079 cm^{-1}, and 1019 cm^{-1} assigned to C-O-H and C-O carbonyl functional groups [38, 39]. The presence of these functional groups in Figure 2(b) as well, especially the O-H hydroxyl groups which are attributed to polyphenols and have previously been reported to present a deterministic part in the silver ions reduction to AgNPs, confirms the successful formulation and capping of AgNPs by the starch extract [40, 41]. Moreover, the decrease in peak intensity of these functional groups observed in Figure 2 is said to indicate the binding of the extract's bimolecular components such as glycogen or cellulose polysaccharide polymers on the surface of the AgNPs [42]. It is postulated that these polysaccharide polymers act as surfactants and capping agents that bind to the NPs by either their cysteine residues or by their free amine groups providing colloidal stability and preventing aggregation [42, 43]. Additionally, previous studies have reported that biomolecules such as alkynes, alcohols, amines, and phenols all have a strong capacity to interact with metal salts to aid their reduction to NPs [44–46]. From these findings, it can be deduced that the AgNPs were successfully synthesized and stabilized using cowpea porous starch extract as corroborated by the previous literature.

3.1.3. TEM, SEM, and Zeta Potential Analysis. Nanoparticle stability is usually determined by shape, particle size, and surface charge (*zeta* potential) [2]. TEM analysis was able to give a clear morphology and size of AgNPs, while the morphological property of cowpea starch extract was analysed using SEM. Biosynthesized AgNPs appeared spherical with a uniform distribution, ranging from 40–70 nm as depicted in Figures 3(a) and 3(b)), while cowpea porous starch extract appeared spherical, granular, and polygonal in shape as depicted in Figures 3(c) and 3(d). These findings correlate with a previous study reported in [47]. Previous studies have shown that the diameter of plasma membrane pores of most cells ranges from 50–75 nm in size, and thus, the synthesized AgNPs having this size range are significant because it means they would be able to extravasate through the cell membrane of the cancer cells via an endocytosis-mediated mechanism [48]. The synthesized AgNPs displayed good stability as indicated by a *zeta* (Ω) potential measurement of -23.9 ± 1.02 mV (Figure 3(e)). According to previous research, good stability is shown by Ω potential values that are greater than +25 mV or less than −25 mV [49, 50]. Thus, it can be concluded that these findings are in good agreement with the known literature.

3.1.4. Antibacterial Activity Study. The antibacterial activity of the synthesized porous-starch-mediated AgNPs of different Molar (M) concentrations (1 M, 5 M, and 10 M) was investigated against Gram-negative bacteria (*E. coli* and *K. pneumoniae*) and Gram-positive bacteria (*L. monocytogenes* and *S. aureus*) using the disc diffusion method. Figure 4 shows that AgNPs exhibited good antimicrobial activity against both Gram-positive and Gram-negative bacteria. No antimicrobial activity was displayed by the starch; this was expected since starch has never been reported to have any antimicrobial activity [51]. The antimicrobial activity observed in both bacterial strains is said to be due to the released silver cations from AgNPs which behave as bactericidal agents. Even though the main antibacterial activity mechanism of the AgNPs is not yet known, researchers have postulated that the AgNPs bind onto the bacteria's cell surface and interact with the phosphorous and sulphur moieties on the

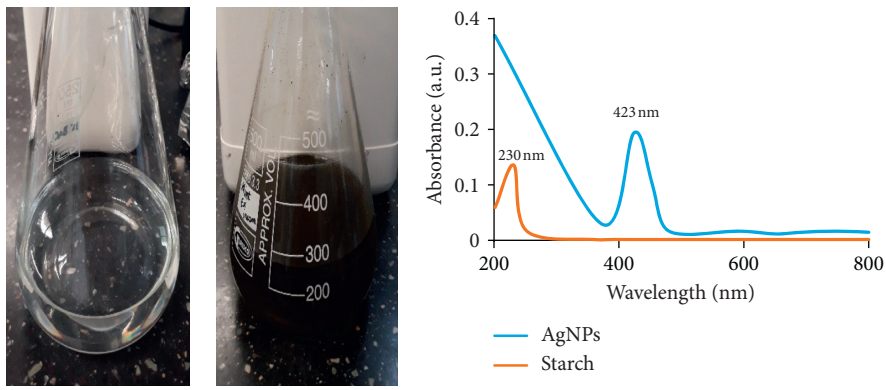

(a) (b) (c)

Figure 1: Formation of porous-starch-mediated AgNPs indicated by positive colour change (dark brown). (a) $AgNO_3$ solution before addition of starch and (b) after addition of starch and (c) UV spectra of synthesized AgNPs and porous starch.

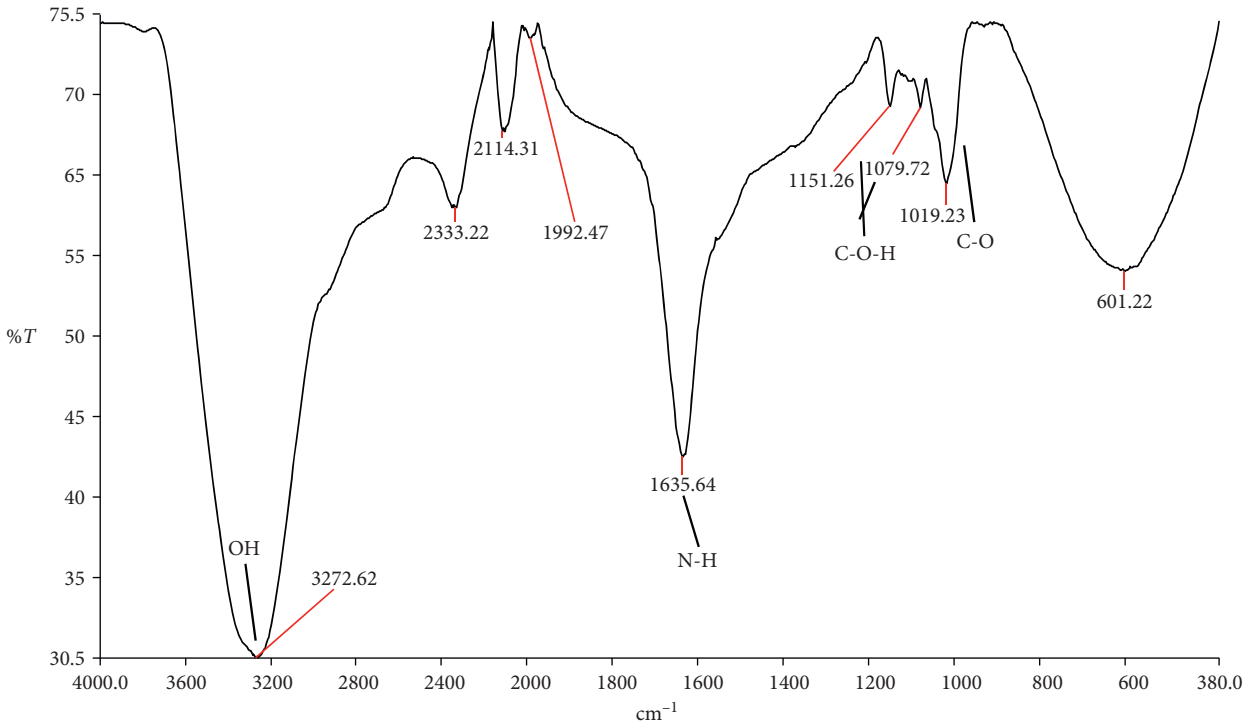

(a)

Figure 2: Continued.

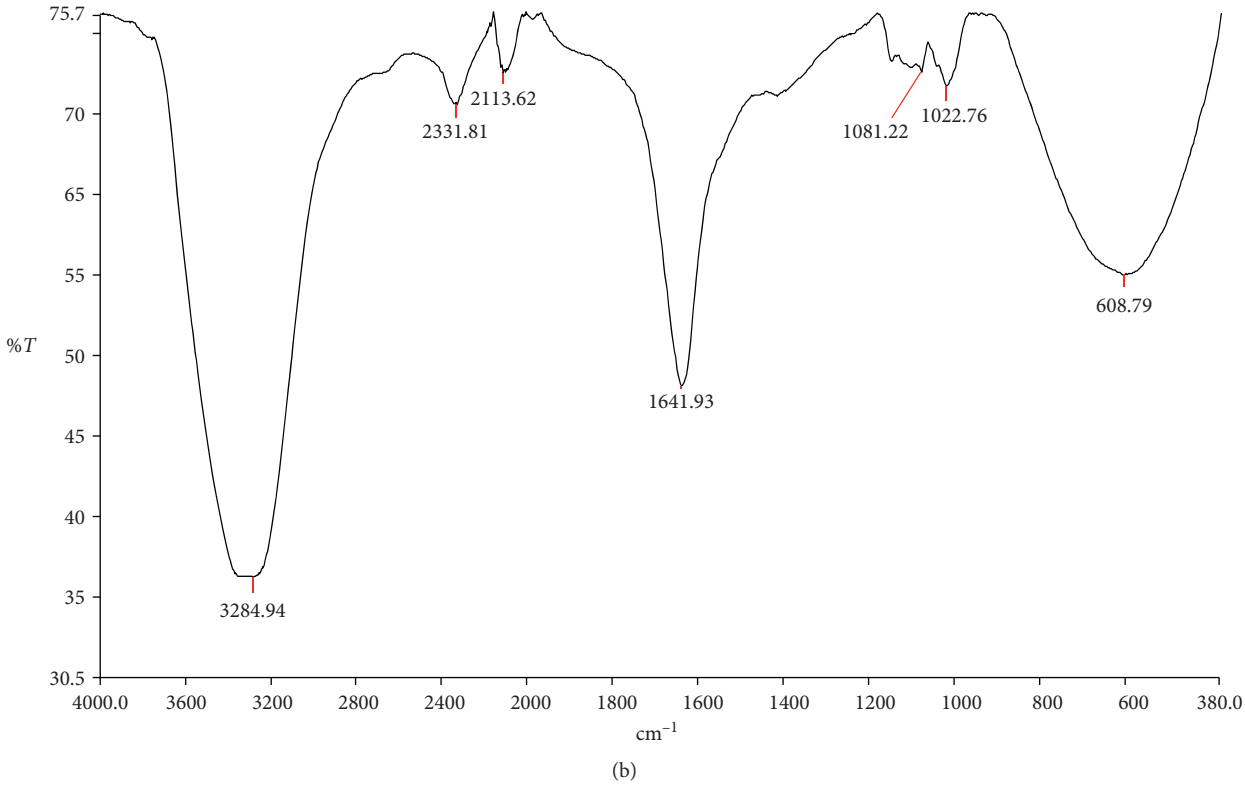

Figure 2: FTIR spectra of (a) cowpea porous starch extract and (b) cowpea-porous-starch-mediated AgNPs.

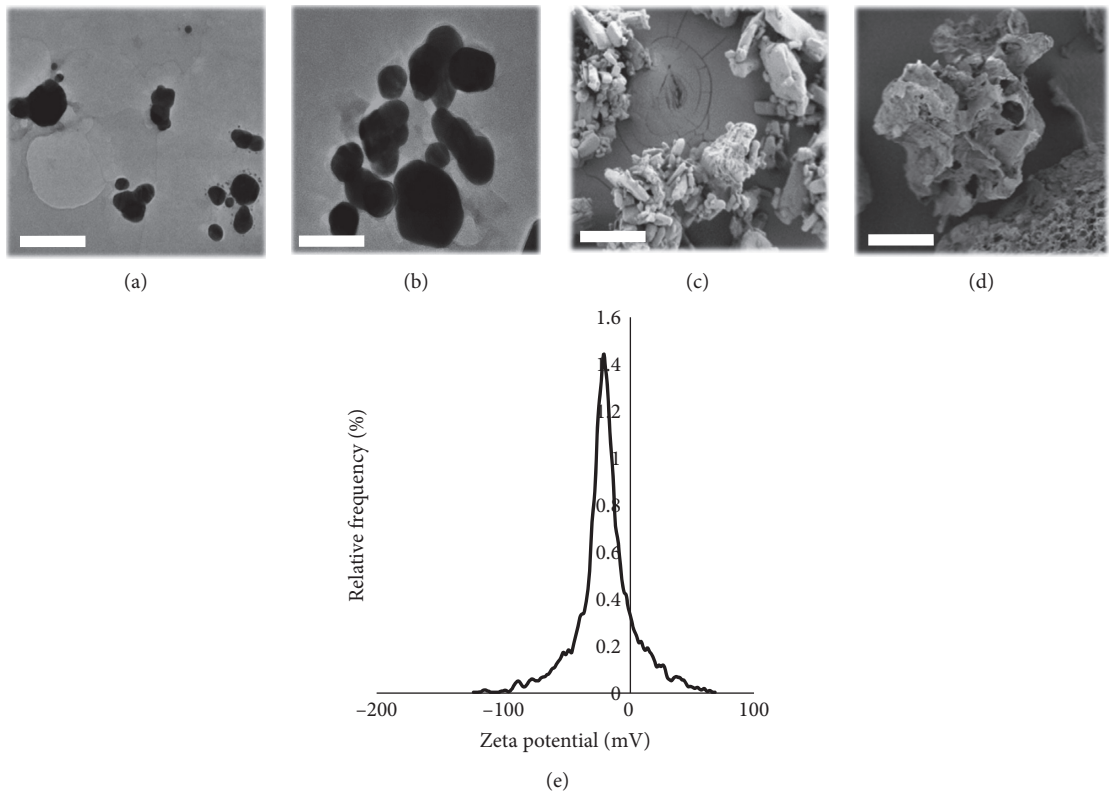

Figure 3: TEM micrographs of starch-mediated AgNPs at (a) 100 nm scale and (b) 10 nm. SEM micrographs of cowpea porous starch at (c) 100 μm scale and (d) 10 μm scale. *Zeta* potential plot of porous-starch-mediated AgNPs (e).

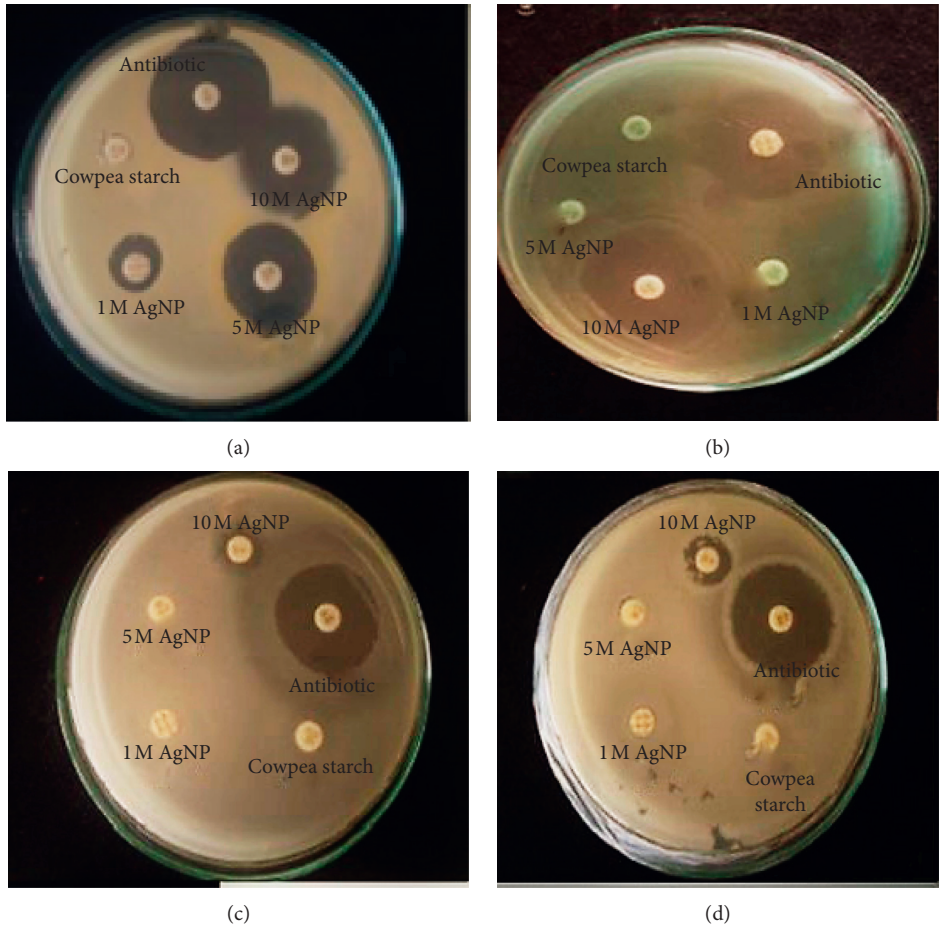

Figure 4: Antimicrobial efficacy of porous-starch-mediated AgNPs and against (a) *E. coli*, (b) *K. pneumonia,* (c) *L. monocytogenes*, and (d) *S. aureus* bacterial strains after exposure to different concentrations of AgNPs. Porous starch extract only (10 Molar) served as a negative control, and antibiotic ciprofloxacin (10 Molar) served as a positive control.

cell membrane leading to metabolism failure which ultimately causes bacterial lysis or apoptosis [52]. This postulation has led to the proposal of several possible AgNP's antibacterial activity mechanisms. These include interference of key metabolic pathways, interference of transcription and translation of protein, and disruption of cell wall synthesis [53]. Hence, it is said that the bacterial growth inhibition not only affects structural constituents but also affects biochemical constituents as well involving enzyme deactivation, cell physiology impairment, and strong ionic charge interaction between silver ions and cell membrane components leading to a synergistic effect against the bacteria causing its death [53, 54].

Figure 4 further shows that AgNPs exhibited higher antimicrobial activity against Gram-negative *E. coli* (18 ± 0.5 mm) over Gram-positive *L. monocytogenes* (6 ± 0.4 mm) after treatment with 10 M AgNP solution. The activity differences can be credited to the diverse properties of each bacterial strain which ultimately constitutes to its mechanism of inhibition [13, 55]. In particular, Gram-positive bacteria are said to have a thick cell wall composition that is hard to be penetrated easily, while Gram-negative bacteria, on the other hand, possess an easily penetrable thin cell wall [11, 56]. The findings are in good agreement with previous reports [11, 55, 57–60]. From Figure 4, it is also observed that both the 1 M and 5 M AgNP solutions did not exhibit any microbial activity in all bacteria except in *E. coli*, whereas the 10 M exhibited good zones of inhibitions in all bacterial strains tested. When the zones of inhibitions were compared with ciprofloxacin (standard antibiotic drug), it was established that the 10 M AgNP solution was as strong as the antibiotic drug against the Gram-negative bacterial strains, while the opposite was true with the Gram-positive bacterial strains. Overall, between the three AgNP concentrations tested, the 10 M showed to be very effective against a range of tested bacterial strains. Table 1 shows in detail the inhibition zones of the AgNPs as measured with a Vernier caliper, as well as the respective minimum inhibitory concentrations which ranged from 5 to 16 mg/l. The lower MIC indicated that the NPs were more potent; hence, a less amount is needed to achieve the desired effect [51, 61]. Previous reports investigating the antimicrobial activity of biosynthesized AgNPs have reported a similar MIC range [55, 62–65]; hence, these findings are in good agreement. In general, the findings suggested these AgNPs as good potential antibacterial agents.

Table 1: Antibacterial activity and MIC of porous-starch-mediated AgNPs against various bacteria.

Bacterial strains	Zone of Inhibition (mm)					
	AgNP concentrations			Controls		
	[1 M]	[5 M]	[10 M]	MIC [mg/l]	Starch [10 M]	Ciprofloxacin [10 M]
(1) *E. coli*	6 ± 0.3	11 ± 0.5	18 ± 0.5	12	0	21 ± 0.0
(2) *K. pneumoniae*	0	0	16 ± 0.2	16	0	20 ± 0.2
(3) *L. monocytogenes*	0	0	6 ± 0.4	5	0	20 ± 0.2
(4) *S. aureus*	0	0	8 ± 0.6	8	0	22 ± 0.3

[a]Amount of AgNPs in 100 μl of deionized water (mg/l): 1 M = 5.35 mg/l; 5 M = 26.75 mg/l; and 10 M = 53.5 mg/l. [b]Data are presented as mean ± SD ($n = 3$). [c]Zero (0) denotes no activity. [d]M denotes Molar.

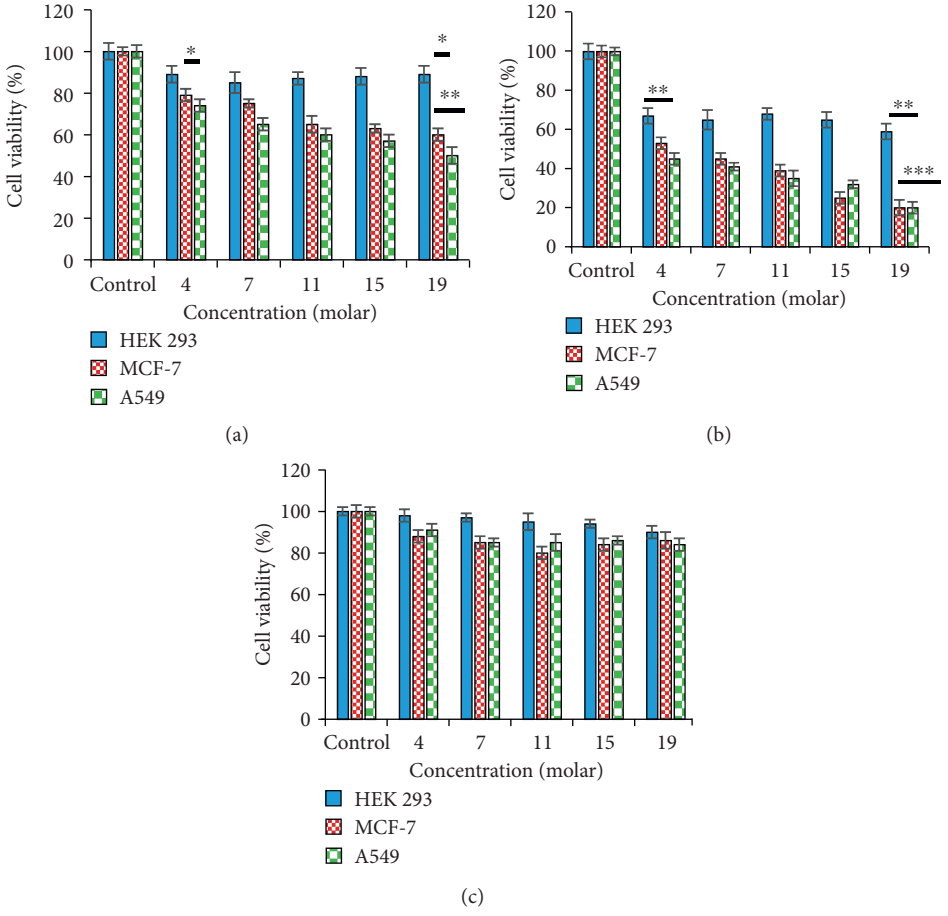

Figure 5: Cell viability studies of (a) porous-starch-mediated AgNPs and (b) $AgNO_3$ and (c) porous starch extract in HEK293, MCF-7, and A459 cells after treatment with different concentrations of 4, 7, 11, 15, and 19 Molar (M). Data are presented as means ± S.D. ($n = 3$). Control: untreated cells. $^{*}p < 0.05$, $^{**}p < 0.01$, $^{***}p < 0.001$, and $^{****}p < 0.0001$ vs. control.

3.1.5. Cell Viability/Cytotoxicity Profile Studies

(1) MTT Assay. The successful application of NPs in cancer therapy applications, particularly in gene delivery, largely depends on their toxicity; therefore, the determination of NPs' cytotoxic profile is vital. The MTT assay which is based on the reduction of the tetrazolium salt, MTT, by living cells to form a blue formazan product which is spectroscopically quantified [30, 66] and reported as a measure of cell viability was employed to assess the cytotoxicity profiles of the synthesized AgNPs (test) against one mammalian noncancer cell line (HEK293) and two cancer cell lines (MCF-7 and A549). The cytotoxicity of porous starch (control) and $AgNO_3$ was also evaluated for comparative studies. The cytotoxicity investigations were carried out at various increasing concentrations of 4, 7, 11, 15, and 19 M on the selected cells. Figure 5(a) shows that the AgNPs elicited moderate cytotoxicity profiles of 40% and 50% against MCF-7 and A549 cancer cells and a very low cytotoxicity profile of 15% against HEK293 cells at the highest dose tested, revealing that their cytotoxicity was cell-specific [67]. This could be due to the highest uptake of these AgNPs by these

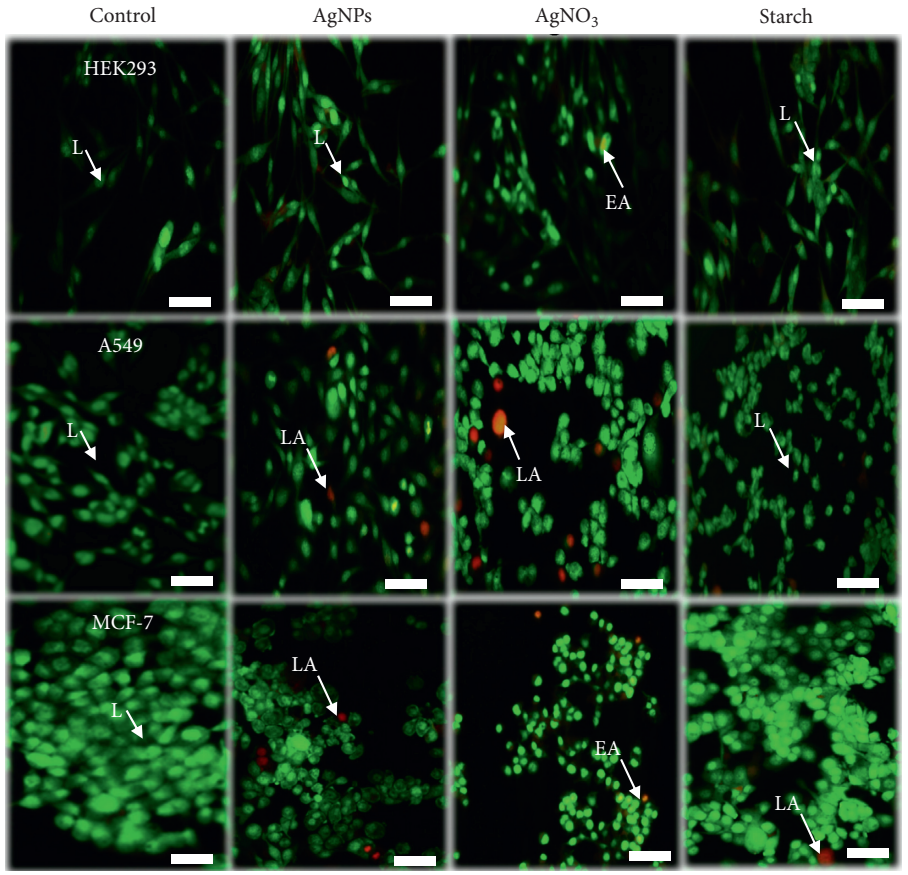

Figure 6: Fluorescence images of HEK293, A459, and MCF-7 cells treated with 10 Molar AgNPs and starch only for 24 hours showing induction of apoptosis. Green = live (L), orange = early apoptotic (EA), and late apoptotic (LA) cells. Scale bar = 100 μm.

Table 2: Apoptotic Indices of AgNPs, $AgNO_3$, and starch in selected cell lines.

Cell lines	Apoptotic Indices			
	Cells only	AgNPs	$AgNO_3$	Starch
HEK293	0.0	0.00	0.01	0.00
A549	0.0	0.10	0.19	0.02
MCF-7	0.0	0.12	0.14	0.08

cells since they have an abnormally high metabolism rate, which leads to their high proliferation which, as a result, makes them more susceptible [68]. It has also been suggested that the cytotoxicity can be credited to the volume-large surface area ratio of AgNPs which enables them to enter the cancer cells easily leading to them to interact with the constituents of the cells and, hence, interrupt many cellular signalling pathways [69]. This disturbance is said to cause an increased influx in the reactive oxygen species (ROS) that lead to oxidative stress [70, 71]. Figure 5(a) further shows that the cytotoxicity of the AgNPs increased as the concentration increased, indicating its dose dependency in both cancer cells. The findings are in good agreement with the previous literature, which accounts for the concentration-dependent cytotoxicity of NPs [55, 67, 72, 73]. Furthermore, similar comparative studies were also conducted using $AgNO_3$ and starch extract only. Figure 5(b) shows that significantly ($p < 0.0001$) higher cytotoxicity profiles of 80% against both MCF-7 and A549 cancer cells and moderate cytotoxicity profile of 40% against HEK293 cells at the highest dose tested were seen after treatment with $AgNO_3$, revealing the non-cell-specificity of this compound as it inhibited both the noncancer and cancer cells. These findings showed that even though this compound showed some degree of anticancer activity, as also previously reported in [74], it cannot make a good anticancer therapeutic system on its own, since it affects both normal and cancer cells. An ideal anticancer agent must be able to elicit its therapeutic effect on the targeted cancer cells without killing the normal cells [75]. Moreover, significantly lower cytotoxicity profiles of less than 15% across all tested cells and doses were seen after treatment with starch (Figure 5(c)), verifying its nontoxicity. These findings are in good agreement with a previous report which showed that starch is nontoxic and has no growth inhibitory effect on human cells whether cancerous or noncancerous [76].

Overall, between the test AgNPs and their $AgNO_3$ counterpart, the test AgNPs exhibited low cytotoxicity with IC_{50} of41.7, 56.3, and 63.8 μg/ml on HEK293, MCF-7, and A549, respectively. The lower IC_{50} values indicated that the AgNPs were more potent; hence, a less amount is needed to achieve the desired effect, and it is less likely for these to have side effects [77]. From these findings, it can be deduced that

these AgNPs were well tolerated by all cells tested even at the highest concentration tested. Furthermore, it can also be postulated that the inclusion of starch into the nanoparticles greatly improved their overall cytotoxicity and biocompatibility, thus indicating these AgNPs as great anticancer potential therapeutics.

(2) Apoptosis Assay. Generally, after the cells have been treated with potential toxicants (e.g., NPs), apoptosis ("programmed cell death") can occur as a response to this external entity. [78]. During apoptosis, the cells undergo morphological changes that can be observed microscopically such as nuclear fragmentation and shrinkage of the cytoplasm. To capture these changes, a combination of fluorescence microscopy and AO/ETB double staining was used [31]. Figure 6 shows that the test AgNPs induced some level of apoptosis as determined by low apoptosis indices (AI) (<1.5) as seen in Table 2, and the apoptosis or morphological changes were most noticeable in the cancer cells (MCF-7 and A549) which appeared to have lost their usual shape and appeared round and shrunk, as compared to the control (HEK 293) (untreated cells) which did not show any morphological changes [79].

The apoptosis activity can be attributed to the prooxidant behaviour shown by AgNPs when inside cancer cells, due to the different redox and osmotic state of these cells [80]. It is believed that these AgNPs enter the cells via endocytosis and elicit their anticancer activity in a controlled release manner ultimately improving their bioavailability [81]. The difference between normal cells and cancer cells is said to contribute to reduced toxicity. It is postulated that the imbalance in the redox and osmotic state of cancer cells triggers the conversion AgNPs which further triggers the production of free radicals. This results in increased stress in the endoplasmic reticulum and disrupts the mitochondrial membrane which leads to mitochondrial proteins leakage which triggers apoptosis via caspase activation [82, 83]. These cellular disruptions then initiate damage to the DNA triggering cell cycle arrest which eventually leads to cell death. This is supported by the nonearly apoptotic cells which appeared light yellow and late apoptotic cells which appeared orange as seen in Figure 6. Hence, the data suggest that porous-starch-mediated AgNPs were able to alter the cell cycle in a dose-dependent manner which explains the observed link between cell death and cell growth inhibition.

4. Conclusions

This study investigated the antimicrobial and anticancer potential of porous-starch-mediated silver nanoparticles. These AgNPs were successfully synthesized using a porous starch extract from cowpea and were very stable. They all showed good antibacterial activity against four tested Gram-positive and Gram-negative bacterial strains. When tested on noncancer and cancerous cell lines, these AgNPs were well tolerated as indicated by a cell viability greater than 50% and low apoptotic indices (<0.2) at the highest dose tested.

Data Availability

Supporting data/figures are available from corresponding author upon request.

Conflicts of Interest

The authors declare that there are no conflicts of interest regarding the publication of this paper.

Acknowledgments

The Durban University of Technology is acknowledged for the support.

Supplementary Materials

Nonlinear regression plot of cell viability (%) versus NP concentration (μg/ml) of (a) HEK 293, (b) MCF-7, and (c) A549 cells. (*Supplementary Materials*)

References

[1] T. K. Mackey, B. A. Liang, R. Cuomo, R. Hafen, K. C. Brouwer, and D. E. Lee, "Emerging and reemerging neglected tropical diseases: a review of key characteristics, risk factors, and the policy and innovation environment," *Clinical Microbiology Reviews*, vol. 27, no. 4, pp. 949–979, 2014.

[2] J. Akinyelu and M. Singh, "Folate-tagged chitosan-functionalized gold nanoparticles for enhanced delivery of 5-fluorouracil to cancer cells," *Applied Nanoscience*, vol. 9, no. 1, pp. 7–17, 2019.

[3] F. Qi, L. Zhao, A. Zhou et al., "The advantages of using traditional Chinese medicine as an adjunctive therapy in the whole course of cancer treatment instead of only terminal stage of cancer," *BioScience Trends*, vol. 9, no. 1, pp. 16–34, 2015.

[4] M. Akram, M. Iqbal, M. Daniyal, and A. U. Khan, "Awareness and current knowledge of breast cancer," *Biological Research*, vol. 50, no. 1, pp. 1–23, 2017.

[5] S. Bisht, M. Mizuma, G. Feldmann et al., "Systemic administration of polymeric nanoparticle-encapsulated curcumin (NanoCurc) blocks tumor growth and metastases in preclinical models of pancreatic cancer," *Molecular Cancer Therapeutics*, vol. 9, no. 8, pp. 2255–2264, 2010.

[6] N. Vasan, J. Baselga, and D. M. Hyman, "A view on drug resistance in cancer," *Nature*, vol. 575, no. 7782, pp. 299–309, 2019.

[7] G. M. Raghavendra, J. Jung, D. kim, and J. Seo, "Step-reduced synthesis of starch-silver nanoparticles," *International Journal of Biological Macromolecules*, vol. 86, pp. 126–128, 2016.

[8] A. C. Burduşel, O. Gherasim, A. M. Grumezescu, F. A. MogoantăL, and E. Andronescu, "Biomedical applications of silver nanoparticles: an up-to-date overview," *Nanomaterials*, vol. 8, no. 9, p. 681, 2018.

[9] S. Lee and B.-H. Jun, "Silver nanoparticles: synthesis and application for nanomedicine," *International Journal of Molecular Sciences*, vol. 20, no. 4, p. 865, 2019.

[10] T. Prasad and E. Elumalai, "Biofabrication of Ag nanoparticles using Moringa oleifera leaf extract and their antimicrobial

activity," *Asian Pacific Journal of Tropical Biomedicine*, vol. 1, no. 6, pp. 439–442, 2011.

[11] Y. N. Slavin, J. Asnis, U. O. Häfeli, and H. Bach, "Metal nanoparticles: understanding the mechanisms behind antibacterial activity," *Journal of Nanobiotechnology*, vol. 15, no. 1, p. 65, 2017.

[12] M. Seong and D. G. Lee, "Silver nanoparticles against *Salmonella enterica* serotype typhimurium: role of inner membrane dysfunction," *Current Microbiology*, vol. 74, no. 6, pp. 661–670, 2017.

[13] X. Wang, L. Yuan, H. Deng, and Z. Zhang, "Structural characterization and stability study of green synthesized starch stabilized silver nanoparticles loaded with Isoorientin," *Food Chemistry*, vol. 338, Article ID 127807, 2021.

[14] V. Demchenko, S. Riabov, S. Sinelnikov, O. Radchenko, S. Kobylinskyi, and N. Rybalchenko, "Novel approach to synthesis of silver nanoparticles in interpolyelectrolyte complexes based on pectin, chitosan, starch and their derivatives," *Carbohydrate Polymers*, vol. 242, Article ID 116431, 2020.

[15] T. Tinus, M. Damour Van Riel, V. van Riel, and P. A. Sopade, "Particle size-starch-protein digestibility relationships in cowpea (Vigna unguiculata)," *Journal of Food Engineering*, vol. 113, no. 2, pp. 254–264, 2012.

[16] T. S. Naiker, A. Gerrano, and J. Mellem, "Physicochemical properties of flour produced from different cowpea (Vigna unguiculata) cultivars of Southern African origin," *Journal of Food Science and Technology*, vol. 56, no. 3, pp. 1541–1550, 2019.

[17] F. Folmer, U. Basavaraju, M. Jaspars et al., "Anticancer effects of bioactive berry compounds," *Phytochemistry Reviews*, vol. 13, no. 1, pp. 295–322, 2014.

[18] L. O. Ojwang, N. Banerjee, G. D. Noratto et al., "Polyphenolic extracts from cowpea (Vigna unguiculata) protect colonic myofibroblasts (CCD18Co cells) from lipopolysaccharide (LPS)-induced inflammation—modulation of microRNA 126," *Food & Function*, vol. 6, no. 1, pp. 145–153, 2015.

[19] P. Patel, P. Agarwal, S. Kanawaria, S. Kachhwaha, and S. L. Kothari, "Plant-based synthesis of silver nanoparticles and their characterization," *Nanotechnology and Plant Sciences*, vol. 288, pp. 271–288, 2015.

[20] S. Rajeshkuma and L. V. Bharath, "Mechanism of plant-mediated synthesis of silver nanoparticles—a review on biomolecules involved," *Characterization and Antibacterial Chemico-Biological Interactions*, vol. 273, pp. 219–227, 2017.

[21] Y. Ding, Q. Lin, and J. Kan, "Development and characteristics nanoscale retrograded starch as an encapsulating agent for colon-specific drug delivery," *Colloids and Surfaces B: Biointerfaces*, vol. 171, pp. 656–667, 2018.

[22] M. Sujka, U. Pankiewicz, R. Kowalski, K. Nowosad, and A. Noszczyk-Nowak, "Porous starch and its application in drug delivery systems," *Polymers in Medicine*, vol. 48, no. 1, pp. 25–29, 2018.

[23] A. G. Barroso and N. L. del Mastro, "Physicochemical characterization of irradiated arrowroot starch," *Radiation Physics and Chemistry*, vol. 158, pp. 194–198, 2019.

[24] G. A. Annor, M. Marcone, E. Bertoft, and K. Seetharaman, "In vitro starch digestibility and expected glycemic index of kodo millet (Paspalum scrobiculatum) as affected by starch-protein-lipid interactions," *Cereal Chemistry Journal*, vol. 90, no. 3, pp. 211–217, 2013.

[25] S. M. Yakout and A. A. Mostafa, "A novel green synthesis of silver nanoparticles using soluble starch and its antibacterial activity," *International Journal of Clinical and Experimental Medicine*, vol. 8, no. 3, p. 3538, 2015.

[26] L. G. Matasyoh, J. C. Matasyoh, F. N. Wachira, M. G. Kinyua, A. W. T. Muigai, and T. K. Mukiama, "Chemical composition and antimicrobial activity of the essential oil of Ocimum gratissimum L. growing in Eastern Kenya," *African Journal of Biotechnology*, vol. 6, no. 6, 2007.

[27] M. S. Rappé, S. A. Connon, K. L. Vergin, and S. J. Giovannoni, "Cultivation of the ubiquitous SAR11 marine bacterioplankton clade," *Nature*, vol. 418, no. 6898, pp. 630–633, 2002.

[28] M. Balouiri, M. Sadiki, and S. K. Ibnsouda, "Methods for in vitro evaluating antimicrobial activity: a review," *Journal of Pharmaceutical Analysis*, vol. 6, no. 2, pp. 71–79, 2016.

[29] J. Eloff, "A sensitive and quick microplate method to determine the minimal inhibitory concentration of plant extracts for bacteria," *Planta Medica*, vol. 64, no. 08, pp. 711–713, 1998.

[30] M. Singh and M. Ariatti, "Targeted gene delivery into HepG2 cells using complexes containing DNA, cationized asialoorosomucoid and activated cationic liposomes," *Journal of Controlled Release*, vol. 92, no. 3, pp. 383–394, 2003.

[31] F. Maiyo and M. Singh, "Folate-targeted mRNA Delivery using chitosan-functionalized selenium nanoparticles: potential in cancer immunotherapy," *Pharmaceuticals*, vol. 12, no. 4, p. 164, 2019.

[32] S. Mohanty, S. Mishra, P. Jena, B. Jacob, B. Sarkar, and A. Sonawane, "An investigation on the antibacterial, cytotoxic, and antibiofilm efficacy of starch-stabilized silver nanoparticles," *Nanomedicine: Nanotechnology, Biology and Medicine*, vol. 8, no. 6, pp. 916–924, 2012.

[33] M. Grzelczak, J. Vermant, E. M. Furst, and L. M. Liz-Marzán, "Directed self-assembly of nanoparticles," *ACS Nano*, vol. 4, no. 7, pp. 3591–3605, 2010.

[34] T. I. Shabatina, A. A. Belyaev, and G. B. Sergeev, "Self-assembled nanostructures in silver-cholesterol and silver-thiocholesterol systems," *BioNanoScience*, vol. 3, no. 3, pp. 289–294, 2013.

[35] J.-Y. Xin, Y. Wang, T. Liu, K. Lin, L. Chang, and C.-G. Xia, "Biosysthesis of corn starch palmitate by lipase novozym 435," *International Journal of Molecular Sciences*, vol. 13, no. 6, pp. 7226–7236, 2012.

[36] M. Ghaffari-Moghaddam, R. Hadi-Dabanlou, M. Khajeh, M. Rakhshanipour, and K. Shameli, "Green synthesis of silver nanoparticles using plant extracts," *Korean Journal of Chemical Engineering*, vol. 31, no. 4, pp. 548–557, 2014.

[37] S. Ahmed, H. Saifullah, M. Ahmad, B. L. Swami, and S. Ikram, "Green synthesis of silver nanoparticles using Azadirachta indica aqueous leaf extract," *Journal of Radiation Research and Applied Sciences*, vol. 9, no. 1, pp. 1–7, 2016.

[38] A. Bankar, B. Joshi, A. R. Kumar, and S. Zinjarde, "Banana peel extract mediated novel route for the synthesis of silver nanoparticles," *Colloids and Surfaces A: Physicochemical and Engineering Aspects*, vol. 368, no. 1–3, pp. 58–63, 2010.

[39] P. Uznanski, J. Zakrzewska, F. Favier, S. Kazmierski, and E. Bryszewska, "Synthesis and characterization of silver nanoparticles from (bis)alkylamine silver carboxylate precursors," *Journal of Nanoparticle Research*, vol. 19, no. 3, p. 121, 2017.

[40] C. Mystrioti, T. D. Xanthopoulou, P. Tsakiridis, N. Papassiopi, and A. Xenidis, "Comparative evaluation of five plant extracts and juices for nanoiron synthesis and application for hexavalent chromium reduction," *Science of The Total Environment*, vol. 539, pp. 105–113, 2016.

[41] N. Thakur, V. G. Gaikar, D. Sen, S. Mazumder, and N. S. Pandita, "Phytosynthesis of silver nanoparticles using

walnut (Juglans regia) bark with characterization of the antibacterial activity against Streptococcus mutans," *Analytical Letters*, vol. 50, no. 4, pp. 690–711, 2017.

[42] D. Nayak, S. Ashe, P. R. Rauta, M. Kumari, and B. Nayak, "Bark extract mediated green synthesis of silver nanoparticles: evaluation of antimicrobial activity and antiproliferative response against osteosarcoma," *Materials Science and Engineering: C*, vol. 58, pp. 44–52, 2016.

[43] G. Vinoj, R. Pati, A. Sonawane, and B. Vaseeharan, "In VitroCytotoxic effects of gold nanoparticles coated with functional acyl homoserine lactone lactonase protein from Bacillus licheniformis and their antibiofilm activity against Proteus species," *Antimicrobial Agents and Chemotherapy*, vol. 59, no. 2, pp. 763–771, 2015.

[44] F. Martinez-Gutierrez, P. L. Olive, A. Banuelos et al., "Synthesis, characterization, and evaluation of antimicrobial and cytotoxic effect of silver and titanium nanoparticles," *Nanomedicine: Nanotechnology, Biology and Medicine*, vol. 6, no. 5, pp. 681–688, 2010.

[45] S. Jain and M. S. Mehata, "Medicinal plant leaf extract and pure flavonoid mediated green synthesis of silver nanoparticles and their enhanced antibacterial property," *Scientific Reports*, vol. 7, no. 1, pp. 158–167, 2017.

[46] R. A. Hamouda, M. H. Hussein, R. A. Abo-elmagd, and S. S. Bawazir, "Synthesis and biological characterization of silver nanoparticles derived from the cyanobacterium Oscillatoria limnetica," *Scientific Reports*, vol. 9, no. 1, p. 13071, 2019.

[47] P. Manivasagan, J. Venkatesan, K. Senthilkumar, K. Sivakumar, and S. K. Kim, "Biosynthesis, antimicrobial and cytotoxic effect of silver nanoparticles using a novel Nocardiopsis sp. MBRC-1," *BioMedical Research Internationa*, vol. 2013, 2013.

[48] E. Sánchez-López, D. Gomes, G. Esteruelas et al., "Metal-based nanoparticles as antimicrobial agents: an overview," *Nanomaterials*, vol. 10, no. 2, p. 292, 2020.

[49] S. Honary and F. Zahir, "Effect of zeta potential on the properties of nano-drug delivery systems - a review (Part 2)," *Tropical Journal of Pharmaceutical Research*, vol. 12, no. 2, pp. 265–273, 2013.

[50] I. Ostolska and M. Wiśniewska, "Application of the zeta potential measurements to explanation of colloidal Cr2O3 stability mechanism in the presence of the ionic polyamino acids," *Colloid and Polymer Science*, vol. 292, no. 10, pp. 2453–2464, 2014.

[51] S. W. Ali, S. Bairagi, and S. Banerjee, "Starch-based antimicrobial materials," *Environmental and Microbial Biotechnology*, vol. 60, pp. 43–60, 2021.

[52] A. Rawani, A. Ghosh, and G. Chandra, "Mosquito larvicidal and antimicrobial activity of synthesized nano-crystalline silver particles using leaves and green berry extract of Solanum nigrum L. (Solanaceae: Solanales)," *Acta Tropica*, vol. 128, no. 3, pp. 613–622, 2013.

[53] M. R. Bindhu and M. Umadevi, "Antibacterial and catalytic activities of green synthesized silver nanoparticles," *Spectrochimica Acta Part A: Molecular and Biomolecular Spectroscopy*, vol. 135, pp. 373–378, 2015.

[54] P. Dubey, I. Matai, S. U. Kumar, A. Sachdev, B. Bhushan, and P. Gopinath, "Perturbation of cellular mechanistic system by silver nanoparticle toxicity: cytotoxic, genotoxic and epigenetic potentials," *Advances in Colloid and Interface Science*, vol. 221, pp. 4–21, 2015.

[55] V. Dhand, L. Soumya, S. Bharadwaj, S. Chakra, D. Bhatt, and B. Sreedhar, "Green synthesis of silver nanoparticles using Coffea arabica seed extract and its antibacterial activity," *Materials Science and Engineering: C*, vol. 58, pp. 36–43, 2016.

[56] A. R. Shahverdi, A. Fakhimi, H. R. Shahverdi, and S. Minaian, "Synthesis and effect of silver nanoparticles on the antibacterial activity of different antibiotics against *Staphylococcus aureus* and *Escherichia coli*," *Nanomedicine: Nanotechnology, Biology and Medicine*, vol. 3, no. 2, pp. 168–171, 2007.

[57] M. Guzman, J. Dille, and S. Godet, "Synthesis and antibacterial activity of silver nanoparticles against Gram-positive and Gram-negative bacteria," *Nanomedicine: Nanotechnology, Biology and Medicine*, vol. 8, no. 1, pp. 37–45, 2012.

[58] M. J. Hajipour, K. M. Fromm, A. Akbar Ashkarran et al., "Antibacterial properties of nanoparticles," *Trends in Biotechnology*, vol. 30, no. 10, pp. 499–511, 2012.

[59] S. Khorrami, A. Zarrabi, M. Khaleghi, M. Danaei, and M. Mozafari, "Selective cytotoxicity of green synthesized silver nanoparticles against the MCF-7 tumor cell line and their enhanced antioxidant and antimicrobial properties," *International Journal of Nanomedicine*, vol. 13, pp. 8013–8024, 2018.

[60] N. Patel, K. Kasumbwe, and L. Mbatha, "Antibacterial screening of gunneraperpensa-mediated silver nanoparticles," *Journal of Nanotechnology*, vol. 2020, Article ID 4508543, 7 pages, 2020.

[61] C. Dipankar and S. Murugan, "The green synthesis, characterization and evaluation of the biological activities of silver nanoparticles synthesized from Iresine herbstii leaf aqueous extracts," *Colloids and Surfaces B: Biointerfaces*, vol. 98, pp. 112–119, 2012.

[62] S. Yasin, L. Liu, and J. Yao, "Biosynthesis of silver nanoparticles by bamboo leaves extract and their antimicrobial activity," *Journal of Fiber Bioengineering and Informatics*, vol. 6, no. 6, pp. 77–84, 2013.

[63] R. W. Raut, V. D. Mendhulkar, and S. B. Kashid, "Photosensitized synthesis of silver nanoparticles using Withania somnifera leaf powder and silver nitrate," *Journal of Photochemistry and Photobiology B: Biology*, vol. 132, pp. 45–55, 2014.

[64] S. Kumar, M. Singh, D. Halder, and A. Mitra, "Mechanistic study of antibacterial activity of biologically synthesized silver nanocolloids," *Colloids and Surfaces A: Physicochemical and Engineering Aspects*, vol. 449, pp. 82–86, 2014.

[65] K. K. H. Anand and B. K. Mandal, "Activity study of biogenic spherical silver nanoparticles towards microbes and oxidants," *Spectrochimica Acta Part A: Molecular and Biomolecular Spectroscopy*, vol. 135, pp. 639–645, 2015.

[66] T. Mosmann, "Rapid colorimetric assay for cellular growth and survival: application to proliferation and cytotoxicity assays," *Journal of Immunological Methods*, vol. 65, no. 1-2, pp. 55–63, 1983.

[67] C. Dong, C. Cao, X. Zhang et al., "Wolfberry fruit (Lycium barbarum) extract mediated novel route for the green synthesis of silver nanoparticles," *Optik*, vol. 130, pp. 162–170, 2017.

[68] R. A. Cairns, I. S. Harris, and T. W. Mak, "Regulation of cancer cell metabolism," *Nature Reviews Cancer*, vol. 11, no. 2, pp. 85–95, 2011.

[69] E. Bressan, L. Ferroni, C. Gardin et al., "Silver nanoparticles and mitochondrial interaction," *International Journal of Dentistry*, vol. 2013, Article ID 312747, 8 pages, 2013.

[70] S. Mohan, O. S. Oluwafemi, S. P. Songca et al., "Synthesis, antibacterial, cytotoxicity and sensing properties of starch-capped silver nanoparticles," *Journal of Molecular Liquids*, vol. 213, pp. 75–81, 2016.

[71] M. Iqbal, H. Zafar, A. Mahmood, M. B. K. Niazi, and M. W. Aslam, "Starch-capped silver nanoparticles impregnated into propylamine-substituted PVA films with improved antibacterial and mechanical properties for wound-bandage applications," *Polymers*, vol. 12, no. 9, p. 2112, 2020.

[72] E.-J. Park, J. Yi, Y. Kim, K. Choi, and K. Park, "Silver nanoparticles induce cytotoxicity by a Trojan-horse type mechanism," *Toxicology in Vitro*, vol. 24, no. 3, pp. 872–878, 2010.

[73] P. Palaniappan, G. Sathishkumar, and R. Sankar, "Fabrication of nano-silver particles using *Cymodocea serrulata* and its cytotoxicity effect against human lung cancer A549 cells line," *Spectrochimica Acta Part A: Molecular and Biomolecular Spectroscopy*, vol. 138, pp. 885–890, 2015.

[74] A. Kaplan, G. Akalin Ciftci, and H. M. Kutlu, "Cytotoxic, antiproliferative and apoptotic effects of silver nitrate against H-ras transformed 5RP7," *Cytotechnology*, vol. 68, no. 5, pp. 1727–1735, 2016.

[75] K. D. Tompkins and A. Thorburn, "Focus: death: Regulation of apoptosis by autophagy to enhance cancer therapy," *The Yale Journal of Biology and Medicine*, vol. 92, no. 4, p. 707, 2019.

[76] R. W.-L. Ma and K. Chapman, "A systematic review of the effect of diet in prostate cancer prevention and treatment," *Journal of Human Nutrition and Dietetics*, vol. 22, no. 3, pp. 187–199, 2009.

[77] E. Damiani, J. A. Solorio, A. P. Doyle, and H. M. Wallace, "How reliable are in vitro IC50 values? Values vary with cytotoxicity assays in human glioblastoma cells," *Toxicology Letters*, vol. 302, pp. 28–34, 2019.

[78] B. Thakur, Y. Kumar, and A. Bhatia, "Programmed necrosis and its role in management of breast cancer," *Pathology-Research and Practice*, vol. 215, no. 11, Article ID 152652, 2019.

[79] S. S. Salem, M. M. G. Fouda, A. Fouda et al., "Antibacterial, cytotoxicity and larvicidal activity of green synthesized selenium nanoparticles using Penicillium corylophilum," *Journal of Cluster Science*, vol. 32, no. 2, pp. 351–361, 2020.

[80] Y. Huang, L. He, W. Liu et al., "Selective cellular uptake and induction of apoptosis of cancer-targeted selenium nanoparticles," *Biomaterials*, vol. 34, no. 29, pp. 7106–7116, 2013.

[81] A. Khurana, S. Tekula, M. A. Saifi, P. Venkatesh, and C. Godugu, "Therapeutic applications of selenium nanoparticles," *Biomedicine & Pharmacotherapy*, vol. 111, pp. 802–812, 2019.

[82] J. Conde, G. Doria, and P. Baptista, "Noble metal nanoparticles applications in cancer," *Journal of Drug Delivery*, vol. 2012, Article ID 751075, 12 pages, 2012.

[83] J. Navarro-Yepes, M. Burns, A. Anandhan et al., "Oxidative stress, redox signaling, and autophagy: cell death versus survival," *Antioxidants & Redox Signaling*, vol. 21, no. 1, pp. 66–85, 2014.